Investigation of ultrasonic propagation in high attenuation porous materials

Abdellah Bouchendouka, Zine El Abiddine Fellah, Cong Truc Nguyen, Erick Ogam, Camille Perrot, Arnaud Duval, Thierry Scotti, Claude L. Depollier

Investigation of ultrasonic propagation in high attenuation porous materials

Abdellah Bouchendouka[1]
Aix Marseille Univ, CNRS, Centrale Marseille, LMA UMR 7031, Marseille, France

Zine El Abiddine Fellah
Aix Marseille Univ, CNRS, Centrale Marseille, LMA UMR 7031, Marseille, France

Cong Truc Nguyen
Univ Gustave Eiffel, Univ Paris Est Creteil, CNRS, UMR 8208, MSME, F-77454 Marne-la-Valléee, France

Eric Ogam
Aix Marseille Univ, CNRS, Centrale Marseille, LMA UMR 7031, Marseille, France

Camille Perrot
Univ Gustave Eiffel, Univ Paris Est Creteil, CNRS, UMR 8208, MSME, F-77454 Marne-la-Valléee, France

Arnaud Duval
Trèves products, services and innovation, 2-4 rue Emile Arqu′es, CS 70017, 51686 Reims Cedex 2, France

Thierry Scotti
Aix Marseille Univ, CNRS, Centrale Marseille, LMA UMR 7031, Marseille, France

Claude Depollier
Acoustics Laboratory of the University of Le Mans (LAUM), UMR 6613, Institut d'Acoustique - Graduate School (IA-GS), CNRS, Le Mans University, Le Mans, France

ABSTRACT

This research examines ultrasonic wave propagation in air-saturated plastic foams used for noise pollution reduction, questioning the effectiveness of current models such as the well known Johnson-Champoux-Allard model at high frequencies. These foams present a challenge for existing models to accurately depict visco-inertial and thermal interactions within their pores. The study highlights the model's failure to align experimental results with theoretical predictions. It introduces novel parameters denoted as Σ *and* V *for viscous effects, and* Σ' *and* V' *for thermal effects, to improve the representation of fluid-sturcture interactions. These parameters suggest a more significant boundary layer effect within the pores than previously considered. This approach aims to provide additional physical context for the principles governing the behavior of highly attenuating porous media and to explore new avenues for material characterization that surpass the limitations of existing models.*

1. INTRODUCTION

The study of linear wave propagation in homogeneous porous media saturated with a viscothermal fluid, such as air, has been a topic of significant interest and comprehensive research efforts [1, 2]. The macroscopic equations for a homogenized medium with a non-deformable solid matrix are derived under the assumption that $\lambda \gg l$, wherein λ represents the wavelength, and l is a typical pore size. This formulation is based on the so-called two-scale asymptotic

[1]bouchendouka@lma.cnrs-mrs.fr

homogenization method [3, 4]. In the context of a rigid solid matrix, the porous material is conceptualized as an effective medium, wherein traditional medium properties are represented by two linear response functions: one indicative of an effective density and the other reflective of an effective bulk modulus [5]. These functions describe fluid-structure interactions at the microscale, predominantly characterized by visco-inertial and thermal exchanges [6].

For the density response function, a widely recognized semi-phenomenological model is articulated through the formula proposed by Johnson *et al.* [7], likewise Champoux and Allard [8], and Lafarge *et al.* [9] provided a formula for the bulk modulus. These formulations are the result of a precise description of both the high and low-frequency limits, grounded on the assumption that relaxation processes (both viscous and thermal) are frozen at high frequencies — implying insufficient time for development — and are relaxed at low frequencies, allowing ample time for full development [10]. The proffered formulas for these limits are well verified across a wide variety of porous materials, as long as the wavelength remains much larger than the pore size.

This paper primarily delves into the high-frequency domain, where factors such as the ideal fluid tortuosity and the viscous and thermal characteristic lengths are paramount. Within this limit, pore walls are perceived as locally plane, and the response functions are expanded into integral power series of viscous and thermal skin depths [11, 12]. The expansion within the Johnson-Champoux-Allard (JCA) model is confined to the second order, encapsulated by terms Λ and Λ'. Third-order terms, denoted as Σ and Σ', were introduced by Kergomard *et al.* [11] and subsequently measured experimentally by Roncen *et al.* [13]. Recent investigation by Bouchendouka *et al.* [12] into the transmission of ultrasonic waves through highly attenuating foams emphasized the necessity of integrating fourth-order terms V and V' for accurate dynamic tortuosity expansion characterizations. While the integration of these terms has harmonized experimental observations with theoretical predictions, their nature remains to be fully determined.

This paper aims to provide additional insight into the rationale behind including these terms with a particular emphasis on viscous phenomena and a brief discussion of thermal effects. The structure of this paper is as follows: Section 2 outlines the fundamental equations employed for defining the various high-frequency parameters. Section 3 addresses the limitations of the JCA model within the high-frequency limit, culminating with a comprehensive conclusion presented in Section 5.

2. BASIC EQUATIONS

Under an excitation of a harmonic source of frequency ω, the dynamics of air within a porous medium are fully charcterized at a microscopic scale by the excess temperature τ, excess pressure p, and velocity $\mathbf{v}$ [9, 14]. Solving the microscopic equations that describe air movement across complex frame geometries proves to be a difficult task. Nevertheless, employing the two-scale asymptotic method facilitates notable simplifications. Following Zhou and Sheng [15], a small parameter ϵ is introduced, enabling the computation of both dynamic viscous permeability and dynamic thermal permeability. This parameter ϵ is represented as the ratio l/L, with l representing a microscopic length akin to the scale of pores, and L a macroscopic length determined by the product of the speed of sound in air $c = \sqrt{K_a/\rho_0}$ and the intrinsic viscous relaxation time $t_\nu = l^2/\nu$, where ν is the kinematic viscosity [9]. It is assumed that $\epsilon \ll 1$, with the wavelength λ aligning in order of magnitude with L, and significantly larger than l. This small parameter ϵ is integrated into the analysis through the well-established homogenization approach, which presumes that the fields describing air motion depend on both a slow scale $\mathbf{x}$ and a fast scale $\mathbf{y} = \epsilon^{-1}\mathbf{x}$. These fields, which represent the solution to the visco-thermal problem, are depicted as a series expansion $\mathbf{f}_\epsilon(\mathbf{x},\mathbf{y}) = \mathbf{f}_0(\mathbf{x},\mathbf{y}) + \epsilon\mathbf{f}_1(\mathbf{x},\mathbf{y}) + \ldots$, while the gradient operator is devided into slow and fast components $\nabla = \nabla_x + \epsilon^{-1}\nabla_y$, accommodating for variations on both micro and macro scales [3, 16, 17]. The application of the two-scale asymptotic method yields

significant insights: (i) the manifestation of an oscillating macroscopic pressure gradient F_p (represented as $-\nabla_x p_0$ in references [9, 15]), which acts on the fluid in a specific direction **e**, (ii) the fluid can be considered incompressible (divergence-free) at the microscopic level. While this paper briefly adresses thermal effects, its primary focus is on investigating the viscous effects. As such, the determination of dynamic permeability is achieved through addressing the canonical problem:

$$\frac{1}{\varepsilon^2(\omega)}\bar{\mathbf{v}} = -\nabla\bar{p} + \nabla^2\bar{\mathbf{v}} + \mathbf{e} \tag{1}$$

$$\nabla.\bar{\mathbf{v}} = 0 \tag{2}$$

$$\bar{\mathbf{v}} = 0, \quad on \quad \partial V \tag{3}$$

The velocity field $\bar{\mathbf{v}}$ is scaled as $\bar{\mathbf{v}} = \eta\mathbf{v}/F_p$, where η is the dynamic viscosity, and $\mathbf{v}$ is the velocity field. The term $\bar{p}$ is related to the excess pressure as $\bar{p} = p/F_p$. The vector **e** is a unit vector pointing to the direction of the applied external force, and $\varepsilon(\omega) = \sqrt{\eta/j\rho\omega}$ is the complex skin depth with $j = \sqrt{-1}$. From darcy's law [9], we can write a general expression defining the dynamic permeability as:

$$k(\omega) = \phi < \bar{\mathbf{v}}.\mathbf{e} >, \tag{4}$$

where $< . >= 1/V\int_V .dV$ is the average operator. If we consider the velocity field $\bar{\mathbf{v}}$ to be divergence-free and has zero normal components on the pore interface, an alternative useful form of Equation (4) can be written as:

$$k(\omega) = \phi < \bar{\mathbf{v}}.\mathbf{E} >, \tag{5}$$

where the field **E** is the solution of an electrical problem, which will be discussed in more details in the next section.

2.1. Ideal fluid problem

At extremely high frequencies, relaxation processes like viscous effects within the pores don't have time to express. Consequently, the saturating fluid may be regarded as an ideal fluid, leading to the omission of the term that describes momentum diffusion compared to the inertial term [18]. Under these circumstances, the problem is similair to that of a conducting fluid permeating a porous medium with an insulating solid matrix [18–20], and can be formulated as:

$$\mathbf{e} = \mathbf{E} + \nabla\phi, \tag{6}$$

$$\nabla.\mathbf{E} = 0, \tag{7}$$

$$\mathbf{E}.\mathbf{n} = 0, \quad on \quad \partial V. \tag{8}$$

Equation (6) represents the so-called Hodge decomposition [19, 21], wherein the unit vector **e** is a sum of a solenoidal field with vanishing normal component on the pore-surface interface ($E_\perp = 0$), and the gradient of a potential. The field **E** can be intepreted as the local electrical field devided by the macroscopic applied potential gradient. This local electrical field bears similarity to the velocity in potential flow, with their relationship expressed as $\bar{\mathbf{v}}_p = \varepsilon^2(\omega)\mathbf{E}$ [18], substituting the velocity field $\bar{\mathbf{v}}$ in Equation (4) with $\bar{\mathbf{v}}_p$. Leveraging the identity (4) or (5), the dynamic permeability is thus characterized as:

$$k(\omega) = \phi\varepsilon^2(\omega)\alpha_\infty^{-1}, \tag{9}$$

where

$$\alpha_\infty = \frac{1}{< \mathbf{E}.\mathbf{e} >} = \frac{< \mathbf{E}.\mathbf{E} >}{< \mathbf{E} > . < \mathbf{E} >}, \tag{10}$$

is the ideal fluid tortuosity, which describes the tortuous path of the pores and is always greater than 1, or equal to 1 for straight cylindrical pores.

2.2. Visco-inertial problem

The previous problem does not account for the no-slip condition at the pore wall due to the assumption that momentum diffusion is neglected, given the insufficient interaction time between the particles themselves and with the pore boundaries. Our focus now shifts to the high-frequency behavior of dynamic permeability, specifically accounting for a small boundary layer thickness (skin depth) near the pore walls. This boundary layer is assumed to be small relative to the pore dimensions, with the pore wall surface appearing as locally flat [18]. The real component of dynamic permeability is attributed to this boundary layer. Consequently, to extract its behaviour, we consider a local coordinate ξ which spans from the pore wall at position $\mathbf{r}_{wall}$ into the bulk domain, defined as $-\xi\mathbf{n} = \mathbf{r} - \mathbf{r}_{wall}$, where $\mathbf{n}$ represents a unit outward-facing normal vector [15]. The influence of the momentum diffusion term, using this local coordinate, is expressed as follows:

$$\frac{\partial^2 \bar{\mathbf{v}}}{\partial \xi^2} = \frac{1}{\varepsilon^2(\omega)}(\bar{\mathbf{v}} - \bar{\mathbf{v}}_p). \tag{11}$$

Using the boundary conditions $\bar{\mathbf{v}} = 0$ when $\xi = 0$, and $\bar{\mathbf{v}} = \bar{\mathbf{v}}_p$ when $\xi \to \infty$, the solution to Equation (11) is:

$$\bar{\mathbf{v}} = \bar{\mathbf{v}}_p(1 - e^{-\xi/\varepsilon(\omega)}) = \varepsilon^2(\omega)\mathbf{E}(1 - e^{-\xi/\varepsilon(\omega)}). \tag{12}$$

The scaled velocity field $\bar{\mathbf{v}}$ represents the summation of a potential part $\bar{\mathbf{v}}_p$, and a small contribution of the boundary layer $-\bar{\mathbf{v}}_p e^{-\xi/\varepsilon(\omega)}$. Assuming that there are no viscous effects except in a small region in the vicinity of the wall, one can write:

$$< -\bar{\mathbf{v}}_p.\mathbf{e}e^{-\xi/\varepsilon(\omega)} >= -\frac{1}{V}\int_S \bar{\mathbf{v}}_p.\mathbf{e}dS \int_0^\infty e^{-\xi/\varepsilon(\omega)}d\xi, \tag{13}$$

$$= -\frac{\varepsilon(\omega)}{V}\int_S \bar{\mathbf{v}}_p.\mathbf{e}dS. \tag{14}$$

Using Equations (5),(12), and (14), we obtain:

$$k(\omega) = \phi\varepsilon^2(\omega)\alpha_\infty^{-1}\left(1 - \frac{2}{\Lambda}\varepsilon(\omega) + O(\varepsilon(\omega)^2)\right), \tag{15}$$

where,

$$\frac{2}{\Lambda} = \frac{\int_S \bar{\mathbf{v}}_p^2 dS}{\int_V \bar{\mathbf{v}}_p^2 dV}. \tag{16}$$

Johnson *et al.* [7] define Λ as the ratio of pore volume over pore surface area, weighted by the potential flow velocity. The physical relevance of Λ diminishes at lower frequencies, as is evident from its definition. Assuming the velocity field across the pore volume as well as the pore surface to be that of a potential flow, this overlooks the minor effects of the boundary layer, an assumption that introduces negligible error. This is particularly true at very high frequencies where the pore surface is perceived as nearly flat. The error in Equation (15) is quantified as $O(\varepsilon(\omega)^2)$, making (15) reliably precise [22]. Nonetheless, it becomes apparent in later discussions that for certain materials, this discrepancy cannot be disregarded. Dynamic permeability is expressed in terms of dynamic tortuosity as follows:

$$k(\omega) = \phi\varepsilon^2(\omega)\alpha(\omega)^{-1}, \tag{17}$$

where

$$\alpha(\omega) = \alpha_\infty \left(1 + \frac{2}{\Lambda}\varepsilon(\omega) + O(\varepsilon(\omega)^2)\right), \tag{18}$$

is the so called Johnson-Koplik-Dashen (JKD) model for describing the visco-inertial interactions inside the porous medium.

2.3. High frequency bulk modulus

Champoux and Allard [8] provided an analogy for thermal interactions, which are accounted for by the dynamic bulk modulus $K(\omega)$:

$$K(\omega) = \gamma P_0 \left[\gamma - (\gamma - 1)\left(1 - \frac{2}{\Lambda'}\varepsilon'(\omega)\right)^{-1}\right], \tag{19}$$

where γ is the adiabatic index, P_0 air equilibrium pressure, and $\varepsilon'(\omega) = \varepsilon(\omega)/\sqrt{P_r}$, where P_r is Prandtl number. The parameter Λ' is analogoues to Λ, but the volume and surface elements are not wheighted by the potential velocity:

$$\frac{2}{\Lambda'} = \frac{\int_S dS}{\int_V dV}. \tag{20}$$

The parameter Λ' is obtained by averaging the excess tempreture τ:

$$\tau = \tau_0(1 - e^{-(\xi/\varepsilon'(\omega)}), \tag{21}$$

where τ_0 is the tempreture of the fluid. For high frequencies, τ_0 is the same everywhere in the pore volume except in a small region near the pore walls. The ratio $\gamma P_0/K(\omega)$ is the so called dynamic compressibility, often labeled as $\beta(\omega)$, which acts as a response function describing thermal effects. Lafarge *et al* [9] provided an interesting relationship between the dynamic compressiblity and a thermal dynamic tortuosity $\alpha'(\omega)$:

$$\beta(\omega) = \gamma - \frac{\gamma - 1}{\alpha'(\omega)}. \tag{22}$$

From Equation (19), it is easy to obtain the following expression for $\alpha'(\omega)$:

$$\alpha'(\omega) = \left(1 + \frac{2}{\Lambda'}\varepsilon'(\omega) + O(\varepsilon'(\omega)^2)\right). \tag{23}$$

From the above Equation we can see that the thermal analogy to the ideal fluid tortuosity α_∞ in the high frequency limit is equal to one. Equations (18) and (23) represent the Johnson-Champoux-Allard (JCA) model which describes the visco-inertial and thermal interactions inside the porous medium for high frequencies.

3. HIGHER ORDER TERMS FOR THE RESPONSE FUNCTIONS

In a recent publication, Bouchendouka *et al.* [12] highlighted the limitations of the JCA model, in the high frequency limit, for accurately describing certain characteristics of graphite polyurethane foams (and more generally very resistive porous materials). This investigation involved analyzing the transmitted signals through these foams within the 70 kHz to 130 kHz frequency spectrum (see Figure 1).

During the fabrication of these foams, graphite particles were incorporated to enhance their fire resistance capabilities [23]. It was observed that these graphite particles not only altered the pore size distribution but also increased the heterogeneity within the polyurethane foam structure. The transmission measurements by these foams revealed an unuasual attenuation

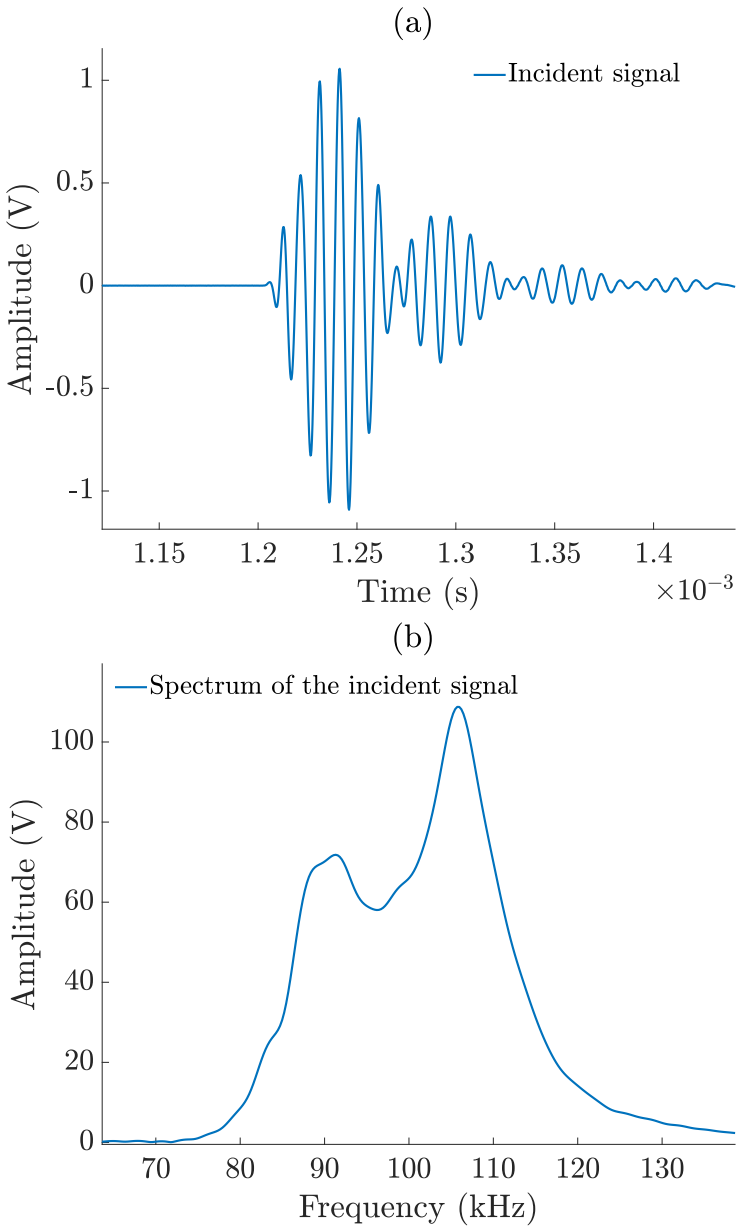

Figure 1: (a) Eperimental incident signal, (b) Spectum of the incident signal

phenomenon (see Figure 2), with a reduction in signal amplitude exceeding 99% [12], rendering these foams highly effective as soundproofing materials. This significant attenuation is attributed to complex physical mechanisms that remain largely unexplained and are not captured by the existing JCA model, which does not match the experimental data. To address these discrepancies, Bouchendouka *et al.* [12] proposed the integration of two new parameters, Σ and V, into the expansion of the dynamic tortuosity $\alpha(\omega)$, along with an additional two parameters, Σ' and V', for the dynamic thermal tortuosity $\alpha'(\omega)$:

$$\alpha(\omega) = \alpha_\infty \left(1 + \frac{2}{\Lambda}\varepsilon(\omega) + \frac{3}{\Sigma}\varepsilon(\omega)^2 + \frac{4}{V}\varepsilon(\omega)^3 + O(\varepsilon(\omega)^4)\right), \tag{24}$$

$$\alpha'(\omega) = \left(1 + \frac{2}{\Lambda'}\varepsilon'(\omega) + \frac{3}{\Sigma'}\varepsilon'(\omega)^2 + \frac{4}{V'}\varepsilon'(\omega)^3 + O(\varepsilon'(\omega)^4)\right). \tag{25}$$

The terms Σ and V relate to viscous effects, with dimensions of surface and volume, respectively. Similarly, Σ' and V', associated with thermal effects, are dimensionalized as surface

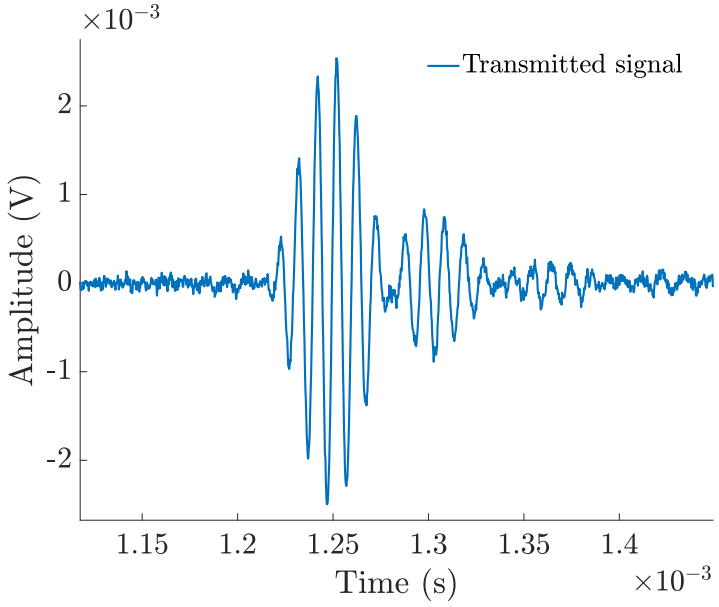

Figure 2: Transmitted signal by a graphite polyurethane foam

and volume. This model has been notably successful in simulating the transmission of signals through the previously mentioned foams (refer to Figure 3). From a physical standpoint, the introduction of surface and volume terms implies an enhancement of the effect of the boundary layer, suggesting that $\delta(\omega)$ is not sufficiently small relative to pore size. Consequently, the applicability of Λ is questioned under circumstances where pore velocities cannot simply be approximated by potential flow, rendering the error in Equation (16) significant. In this case, one needs to raise the following question: Can these foams be accurately described by the divergence-free, long wavelength, high frequency asymptotic models? A straightforward approach to answer this question involves calculating the d/δ ratio, with d representing pore size. A significantly high ratio is indicative of operating within the high-frequency domain, as required by assumptions of the JCA high frequency model. In their thorough investigation into the microstructure of these foams, Nguyen *et al.* [23, 24] estimated an average pore size of $d = 360\mu m \pm 290\mu m$. For a frequency range of 70 kHz to 130 kHz, the results for this ratio are tabulated in Table 1.

	f=70 kHz	f=130 kHz
d=70 μm	12	16
d=360 μm	61	84
d=650 μm	111	151

Table 1: Summary of the ratio d/δ for f=70 kHz-130 kHz and for different statistical values of the average pore size d.

Given the average pore dimension d=360 μm, the calculated ratios of 61 at 70 kHz and 84 at 130 kHz place us squarely within the high-frequency regime. Yet, these values alone may not be sufficiently large to validate the comprehensive application of Equations (18) and (23), hence the need to include higher order terms. Moreover, the wavelengths $\lambda \approx 4900$ μm at 70 kHz and $\lambda \approx 2680$ μm at 130 kHz significantly exceed the pore size, reinforcing the validity of assumptions regarding divergence-free conditions and absence of scattering effects.

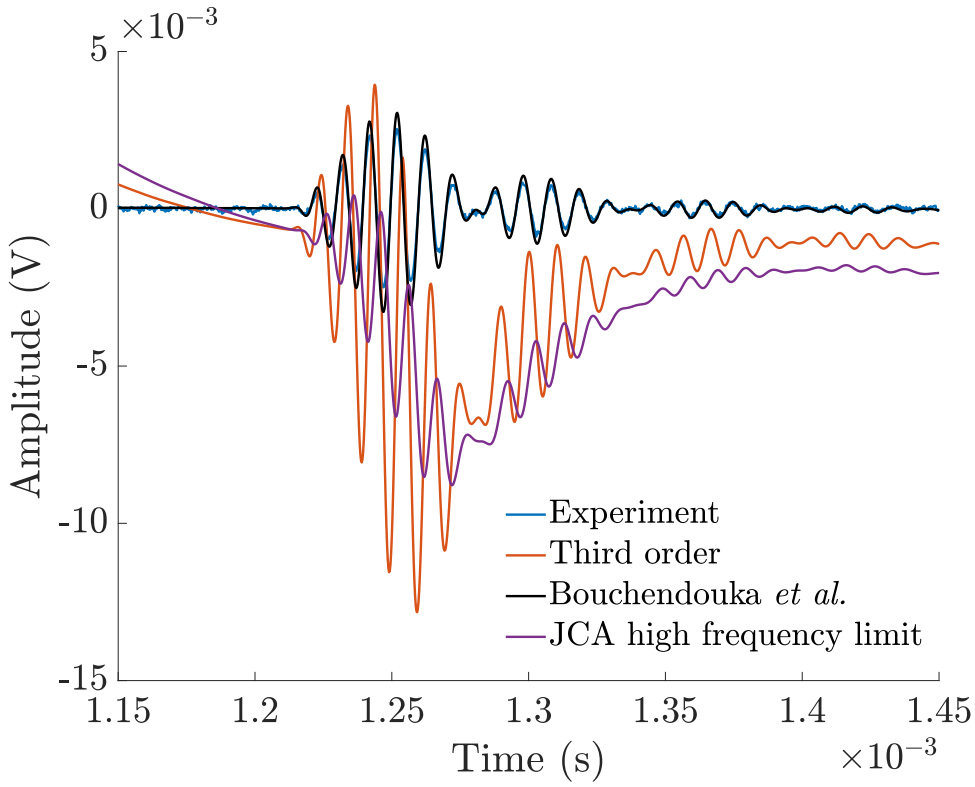

Figure 3: Comparison between the JCA model in high frequencies, third order model, forth order model, and an experimental transmitted signal of a highly attenuated foam.

4. EFFECTIVE RANGES OF HIGHER ORDER PARAMETERS

A practical approach for obtaining the effective ranges of Σ and V where they have a pronounced effect involves representing the entire signal with a singular metric. For this purpose, the peak-to-peak amplitude, referred to as A_{pp}, is chosen as the ideal metric. The value of A_{pp} is calculated by taking the difference between the maximum and minimum values of the simulated transmitted signal, which is obtained by using the transmission coefficient (provided in ref [12]), the incident signal as seen in Figure 1, and computational processing with MATLAB.

In Figure 4, the data is displayed on a semi-logarithmic scale, plotting the derivative of A_{pp} for different values of Λ. These graphs illustrate the variability of (a) $dA_{pp}/d\Sigma$ with respect to Σ, using the third-order model, (b) dA_{pp}/dV with respect to V, in conjunction with a fourth-order model while holding Σ constant at 4000 μm^2, and (c) the parameter Σ is fixed at a value of 40,000 μm^2. These plots are useful for delineating the effective ranges of Σ and V where they have a pronounced effect on wave amplitude and for determining the threshold where increases in these variables cease to have a significant impact.

As Σ and V values increase, we observe that all three curves for Figure 4(a)-(c), seem to follow a similar pattern: they start at lower values, peak around a specific value, and then decline. This representation makes it easy to determine the ranges where Σ and V have the most influence on signal amplitude. The effective range for Σ is identified ,approximately, between 80 μm^2 and 2×10^4 μm^2, whereas V has an effective range from about 500 μm^3 to 10^5 μm^3. If we compare Figure 4(b) and 4(c), it appears that the range for V is independent of Σ. These identified ranges can vary slightly when Λ is altered. In examining the variations of A_{pp} relative to Σ and V, it becomes apparent that V exerts a significantly greater impact on the amplitude. This observation aligns with expectations, given that $\varepsilon(\omega)^2$ pertains exclusively to viscous phenomena (the imaginary component of $\alpha(\omega)$), while $\varepsilon(\omega)^3$ encompasses effects related to both inertia and viscosity (the real and imaginary components of $\alpha(\omega)$).

5. CONCLUSION

To summerize, this paper provided a concise overview on the delineation of high frequency parameters predicated on the assumption that the momentum diffusion process remains frozen at high enough frequencies. It has been shown that in the presence of a small boundary layer near the pore walls, it is possible to expand the dynamic tortuosity into an integral power series of the skin depth, denoted as $\varepsilon(\omega)$. The so-called Johnson-Champoux-Allard model, stops at the order of $\varepsilon(\omega)$, yielding an error magnitude of $O(\varepsilon(\omega)^2)$. This level of accuracy is deemed to be generally satisfactory. Nonetheless, the highly attenuated transmitted signals of certain polydisperse polymeric foams have necessitated the integration of two additional higher-order terms, Σ and V for viscous effects, and Σ' and V' for thermal effects, to enable their characterisation. The requirement to incorporate these terms indicates a marginal increase of the boundary layer, thereby warranting further theoretical and phenomenological research to ascertain the underlying reasons for this augmentation. This investigation paves the way for additional theoretical and experimental investigations, aimed at unravelling the fundamental factors contributing to the high attenuation observed within these foams.

REFERENCES

1. Paolo Bonfiglio and Francesco Pompoli. Inversion problems for determining physical parameters of porous materials: Overview and comparison between different methods. *Acta Acustica united with Acustica*, 99(3):341–351, 2013.
2. Kirill V Horoshenkov. A review of acoustical methods for porous material characterisation. *Int. J. Acoust. Vib*, 22(1):92–103, 2017.
3. Joseph B Keller. Darcy's law for flow in porous media and the two-space method. In *Nonlinear partial differential equations in engineering and applied science*, pages 429–443. Routledge, 2017.
4. Grégoire Allaire. Homogenization and two-scale convergence. *SIAM Journal on Mathematical Analysis*, 23(6):1482–1518, 1992.
5. Jean-François Allard and Noureddine Atalla. *Propagation of sound in porous media: modelling sound absorbing materials*. John Wiley & Sons, 2009.
6. Zine El Abiddine Fellah, C Depollier, and Mohamed Fellah. Application of fractional calculus to the sound waves propagation in rigid porous materials: validation via ultrasonic measurements. *Acta Acustica united with Acustica*, 88(1):34–39, 2002.
7. David Linton Johnson, Joel Koplik, and Roger Dashen. Theory of dynamic permeability and tortuosity in fluid-saturated porous media. *Journal of fluid mechanics*, 176:379–402, 1987.
8. Yvan Champoux and Jean-F Allard. Dynamic tortuosity and bulk modulus in air-saturated porous media. *Journal of applied physics*, 70(4):1975–1979, 1991.
9. Denis Lafarge, Pavel Lemarinier, Jean F Allard, and Viggo Tarnow. Dynamic compressibility of air in porous structures at audible frequencies. *The Journal of the Acoustical Society of America*, 102(4):1995–2006, 1997.
10. Allan D Pierce. *Acoustics: an introduction to its physical principles and applications*. Springer, 2019.
11. Jean Kergomard, Denis Lafarge, and Joël Gilbert. Transients in porous media: Exact and modelled time-domain green's functions. *Acta Acustica united with Acustica*, 99(4):557–571, 2013.
12. Abdellah Bouchendouka, Zine El Abiddine Fellah, Cong Truc Nguyen, Erick Ogam, Camille Perrot, Arnaud Duval, and Claude Depollier. Improving acoustic wave propagation models in highly attenuating porous materials. *The Journal of the Acoustical Society of America*, 155(1):206–217, 2024.

13. Rémi Roncen, Zine El Abiddine Fellah, Estelle Piot, Frank Simon, Erick Ogam, Mohamed Fellah, and Claude Depollier. Inverse identification of a higher order viscous parameter of rigid porous media in the high frequency domain. *The Journal of the Acoustical Society of America*, 145(3):1629–1639, 2019.
14. Michael R Stinson. The propagation of plane sound waves in narrow and wide circular tubes, and generalization to uniform tubes of arbitrary cross-sectional shape. *The Journal of the Acoustical Society of America*, 89(2):550–558, 1991.
15. Min-Yao Zhou and Ping Sheng. First-principles calculations of dynamic permeability in porous media. *Physical Review B*, 39(16):12027, 1989.
16. Robert Burridge and Joseph B Keller. Poroelasticity equations derived from microstructure. *The Journal of the Acoustical Society of America*, 70(4):1140–1146, 1981.
17. George Papanicolau, Alain Bensoussan, and J-L Lions. *Asymptotic analysis for periodic structures*. Elsevier, 1978.
18. Denis Lafarge. *The Equivalent Fluid Model*, chapter 6, pages 153–204. John Wiley & Sons, Ltd, 2009.
19. Marco Avellaneda and Salvatore Torquato. Rigorous link between fluid permeability, electrical conductivity, and relaxation times for transport in porous media. *Physics of Fluids A: Fluid Dynamics*, 3(11):2529–2540, 1991.
20. Andrea Cortis, David MJ Smeulders, Jean Luc Guermond, and Denis Lafarge. Influence of pore roughness on high-frequency permeability. *Physics of fluids*, 15(6):1766–1775, 2003.
21. Günter Schwarz. *Hodge Decomposition-A method for solving boundary value problems*. Springer, 2006.
22. DMJ Smeulders, RLGM Eggels, and MEH Van Dongen. Dynamic permeability: reformulation of theory and new experimental and numerical data. *Journal of Fluid Mechanics*, 245:211–227, 1992.
23. Cong Truc Nguyen. *Acoustic foams with pore size distributions and controlled interconnections: Relationships between structures, properties, fabrication*. PhD thesis, Université Gustave Eiffel, 2021.
24. Cong Truc Nguyen, Johann Guilleminot, Fabrice Detrez, Vincent Langlois, Michel Bornert, Arnaud Duval, and Camille Perrot. Micro-macro acoustic modeling of heterogeneous foams with nucleation perturbation. *SAE International Journal of Advances and Current Practices in Mobility*, 3(2020-01-1526):1068–1074, 2020.

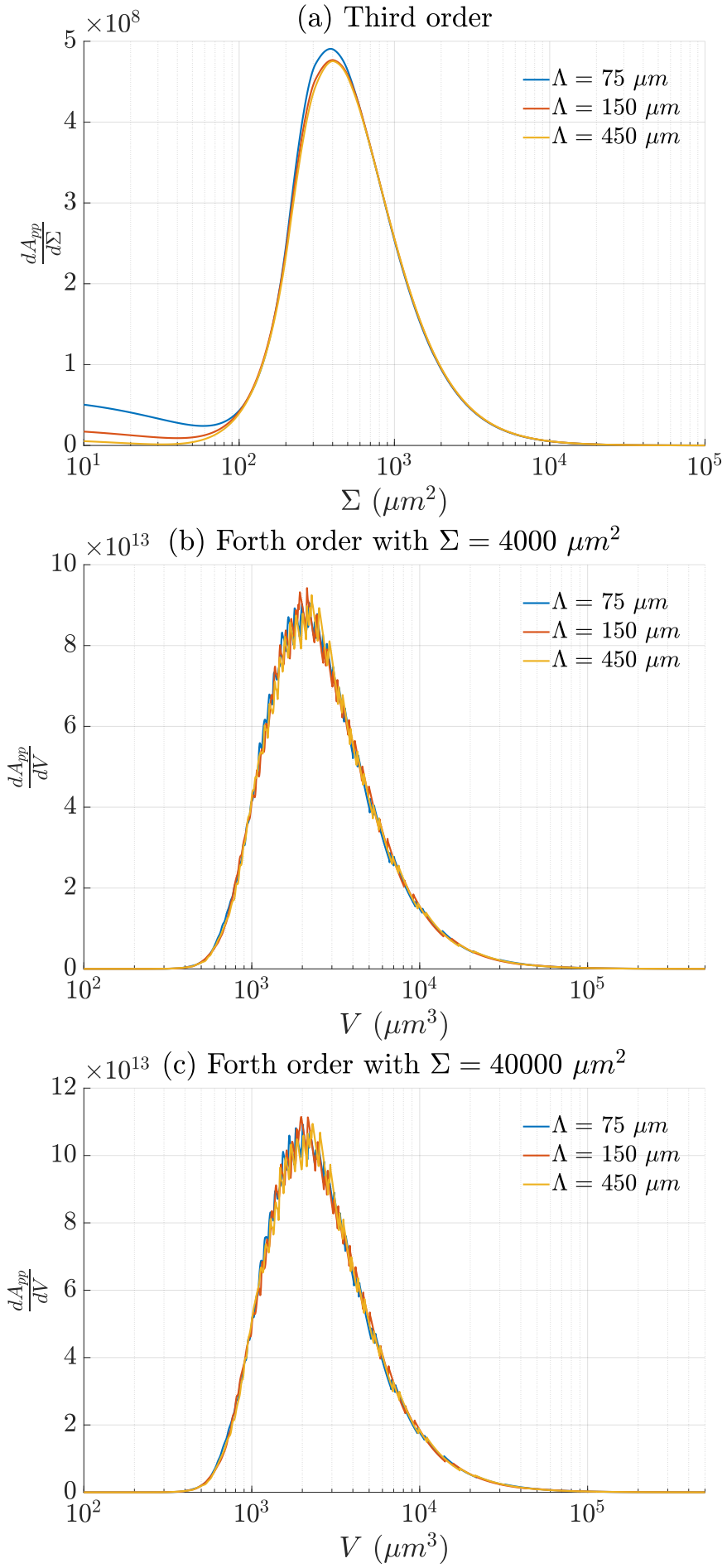

Figure 4: Variation of (a) $dA_{pp}/d\Sigma$ with respect to Σ, (b) dA_{pp}/dV with respect to V for $\Sigma = 4000$ μm^2, (c) for $\Sigma = 40000$ μm^2.